NIH Public Access
Author Manuscript
Cell. Author manuscript; available in PMC 2012 August 03.

Published in final edited form as:
Cell. 2012 February 3; 148(3): 568–582. doi:10.1016/j.cell.2012.01.024.

Ret is a multifunctional co-receptor that integrates diffusible- and contact-axon guidance signals

Dario Bonanomi[1], **Onanong Chivatakarn**[1], **Ge Bai**[1], **Houari Abdesselem**[2], **Karen Lettieri**[1], **Till Marquardt**[3], **Brian A. Pierchala**[2], and **Samuel L. Pfaff**[1,*]

[1]Howard Hughes Medical Institute and Gene Expression Laboratory, The Salk Institute for Biological Studies, La Jolla, CA 92037, USA

[2]Department of Biologic and Materials Sciences, The University of Michigan School of Dentistry, Ann Arbor, MI 48109, USA

[3]Developmental Neurobiology Laboratory, European Neuroscience Institute-Göttingen, Göttingen, Germany

SUMMARY

Growing axons encounter multiple guidance cues, but it is unclear how separate signals are resolved and integrated into coherent instructions for growth cone navigation. We report that glycosylphosphatidylinositol (GPI)-anchored ephrin-As function as “reverse” signaling receptors for motor axons when contacted by transmembrane EphAs present in the dorsal limb. Ephrin-A receptors are thought to depend on transmembrane co-receptors for transmitting signals intracellularly. We show that the receptor tyrosine kinase Ret is required for motor axon attraction mediated by ephrin-A reverse signaling. Ret also mediates GPI-anchored GFRα1 signaling in response to GDNF, a diffusible chemoattractant in the limb - indicating that Ret is a multifunctional co-receptor for guidance molecules. Axons respond synergistically to co-activation by GDNF and EphA ligands and these cooperative interactions are gated by GFRα1 levels. Our studies uncover a hierarchical GPI-receptor signaling network that is constructed from combinatorial components and integrated through Ret using ligand coincidence detection.

Keywords

Motor neuron; axon guidance; Ret; EphA; ephrin-A; coincidence detection; chemoattraction; GFRα1; GDNF

INTRODUCTION

The basic framework for neuronal connections is set during embryonic development using guided axonal growth to form the underlying circuits for complex behaviors. Axon navigation is regulated by a relatively small number of guidance receptors and extracellular signals, yet it occurs with remarkable precision and generates immensely complex wiring patterns (Dickson, 2002). Multiple cues are simultaneously monitored by axons, which

© 2012 Elsevier Inc. All rights reserved.

*Corresponding author: Samuel L. Pfaff, PhD, Investigator, Howard Hughes Medical Institute, Professor, Gene Expression Laboratory, Salk Institute, 10010 North Torrey Pines Rd, La Jolla CA 92037 USA, pfaff@salk.edu, 858-453-4100 x2018.

Publisher's Disclaimer: This is a PDF file of an unedited manuscript that has been accepted for publication. As a service to our customers we are providing this early version of the manuscript. The manuscript will undergo copyediting, typesetting, and review of the resulting proof before it is published in its final citable form. Please note that during the production process errors may be discovered which could affect the content, and all legal disclaimers that apply to the journal pertain.

NIH-PA Author Manuscript
NIH-PA Author Manuscript
NIH-PA Author Manuscript

NIH-PA Author Manuscript

NIH-PA Author Manuscript

NIH-PA Author Manuscript

integrate these signals into coherent instructions for directional growth. Nevertheless, how co-signaling is integrated and the way this is leveraged to improve axon targeting remains poorly understood.

The topographic projection of motor axons into the limb musculature is under the control of multiple signaling pathways that drive the assembly of a seemingly simple binary map: motor neurons located in the lateral division of the lateral motor column (LMC_L) send axons to the dorsal limb, while neurons of the medial division (LMC_M) select a ventral trajectory (Figure 1A) (Bonanomi and Pfaff, 2010; Landmesser, 2001). The ephrin:Eph system of membrane-tethered ligands and receptors lies at the core of the decision-making process of motor axons at the base of the limb (Eberhart et al., 2002; Helmbacher et al., 2000; Kania and Jessell, 2003; ; Luria et al., 2008). Glycosylphosphatidylinositol (GPI)-anchored (class A) and transmembrane (class B) ephrins bind preferentially to their membrane-spanning EphA and EphB tyrosine kinase receptors, respectively. This contact-mediated signaling system operates bidirectionally so that biological outputs are transmitted by the kinase domains of the Eph receptors in a classical “forward” signaling mode and by the ephrins in a “reverse” signaling mode (Pasquale, 2008).

A further layer of complexity derives from the coexpression of ephrin and Eph in the same cell, as observed for LMC_L neurons (Hornberger et al., 1999; Konstantinova et al., 2007; Marquardt et al., 2005). Futile cis-interactions between EphA and ephrin-A are prevented by lateral segregation of the two proteins into distinct membrane subcompartments, allowing the EphAs and ephrin-As to signal independently upon interactions with their cognate ligands (Marquardt et al., 2005). In motor axons, bidirectional ephrin-A:EphA signaling elicits axonal responses that have the opposite polarity: EphA forward signaling triggers repulsion, whereas ephrin-A reverse signaling promotes the axonal growth of cultured neurons (Figure 1D). However, it is unclear whether attractive ephrin-A reverse signaling plays an instructive role in motor axon navigation *in vivo*. It is also unclear why reverse signaling in motor neurons promotes growth whereas ephrin-A reverse signaling in retinal ganglion neurons causes axon repulsion (Lim et al., 2008; Rashid et al., 2005). Because GPI-anchored ephrin-As do not span the plasma membrane, it is assumed they must associate with transmembrane co-receptors to elicit intracellular signaling. The neurotrophin receptors p75 and TrkB are thought to mediate the repulsive effects of ephrin-A in axons and secondary branches of retinal neurons (Lim et al., 2008; Marler et al., 2008). Thus ephrin-A reverse signaling is capable of triggering attractive and repulsive responses, which could rely on different co-receptors.

We investigated ephrin-A reverse signaling in the context of the other guidance systems that control the dorsoventral projection of motor neurons into the limb - a decision that underlies the ability to control flexion and extension movements. We show that *in vivo* ephrin-A reverse signaling is critical for attraction of LMC_L motor neurons into the dorsal limb and is mediated by Ret - a transmembrane tyrosine kinase co-receptor that transmits glial derived neurotrophin factor (GDNF) signaling upon interaction with the ligand-binding GPI-receptor GFRα1. Our data shows that Ret is positioned at a key nodal point for integrating guidance cues by functioning as a coincident detector to amplify axon growth signaling where GDNF and EphA are both present.

RESULTS

Coordination of ephrin-A forward and reverse signaling enhances boundary discrimination

The expression of ephrin-A and EphA on motor axons and hindlimb mesenchyme was surveyed in e11.5 transgenic mouse embryos that express GFP under the control of the motor neuron-specific Hb9 promoter (Lee et al., 2004). In agreement with previous reports,

NIH-PA Author Manuscript

NIH-PA Author Manuscript

NIH-PA Author Manuscript

dorsally-projecting LMC_L axons coexpressed both ephrin-A2/5 and EphA4. In contrast, the limb tissue displayed segregated expression of these proteins: ephrin-A2/5 were high ventrally whereas dorsal cells had EphAs (Figure 1A–D; Figure S1A–C) (references in Bonanomi and Pfaff, 2010). Consequently, Ephrin-A^+/$EphA4^+$ LMC_L axons traverse a broad domain of $EphA^+$ cells in the dorsal limb (Figure 1C). In principle, LMC_L neurons might be subjected to a combination of "push-pull" attractive and repulsive signaling at the base of the limb. The EphA4 receptor in LMC_L axons should signal repulsion from the ephrin-rich ventral limb, whereas ephrin-As should reverse-signal attraction toward the EphA-rich dorsal limb (Figure 1D).

We sought to study the coordination of ephrin-A:EphA forward and reverse signaling in a simplified experimental paradigm that excludes the contribution of other signals present in the limb. The dorsoventral expression of ephrin-As and EphAs was mimicked by culturing lumbar motor neurons on alternating stripes of: EphA7-Fc/ephrin-A5-Fc, control IgG-Fc/ephrin-A5-Fc, EphA7-Fc/IgG-Fc or IgG-Fc/IgG-Fc (Figure 1E–I). We chose EphA7 because it binds strongly to virtually all ephrin-As, but not ephrin-Bs (Flanagan and Vanderhaeghen, 1998) and it is expressed by the dorsal limb mesenchyme (Figure S1C). The majority of axons in these cultures were derived from $EphA4^+$ LMC_L neurons (Figure S1D–F). Motor axons did not exhibit a growth preference on control IgG-Fc/IgG-Fc stripes but were repelled from ephrin-A5-Fc stripes in both IgG-Fc/ephrin-A5-Fc and EphA7-Fc/ephrin-A5-Fc cultures (Figure 1E–I). While EphA7-Fc that activates ephrin-A reverse signaling did not trigger preferential axon growth when paired to permissive IgG-Fc substrate (EphA7-Fc/IgG-Fc stripes) (Figure 1I), it significantly enhanced directional growth when coupled with ephrin-A5-Fc substrate (EphA7-Fc/ephrin-A5-Fc stripes) (Figure 1G–I). Thus, the synchronization of growth-promoting (reverse) and repulsive (forward) ephrin-A signaling enhances the selective choices of motor axons when confronting adjacent domains of EphA and ephrin-A ligands - a situation found in the limb.

Ephrin-A reverse signaling is instructive for motor axon guidance *in vivo*

To determine the *in vivo* contribution of ephrin-As to specific motor axon projections, we analyzed *ephrin-A2* (*Efna2*) and *ephrin-A5* (*Efna5*) knockout mice. The cumulative expression of ephrin-As was markedly reduced in LMC motor neurons and hindlimb tissues of $Efna2^{-/-};Efna5^{-/-}$ mutants, indicating that ephrin-A2 and ephrin-A5 are the two main ephrin-A isoforms at the time of dorsoventral guidance (Figure S1G–K). The fidelity of LMC_L projections in $Efna2^{-/-};Efna5^{-/-}$ embryos was assessed by injecting a retrograde-fluorescent tracer in the ventral shank, the target of LMC_M axons, and assigning the divisional identity of labeled motor neurons using specific markers (Figure 1P). Only a few LMC_L neurons (~5%) were labeled in control embryos (Figure J–L, Q), likely reflecting minor inaccuracies of the tracer injection or rare axons that project inappropriately. In contrast, double-mutant $Efna2^{-/-};Efna5^{-/-}$ embryos displayed numerous LMC_L misprojections into the ventral compartment of the limb: ~27% of the ventral tracer-labeled motor neurons inappropriately belonged to the LMC_L division (Figure 1M–O, Q). This LMC_L guidance phenotype was also apparent in mixed homozygous/heterozygous compound mutants $Efna2^{-/-};Efna5^{-/+}$ and $Efna2^{-/+};Efna5^{-/-}$, although with reduced incidence (Figure 1Q). These findings demonstrate that ephrin-A2 and ephrin-A5 genetically-interact and are required for LMC_L axon pathfinding.

Although motor projection defects were observed in *Efna2;Efna5* knockout embryos, it remained unclear whether this reflected the ligand-function of ephrin-As in the ventral limb tissues and/or the receptor-function of ephrin-A in motor neurons. It was impractical to perform tissue specific knockouts using conditional alleles of *Efna2;Efna5*. Therefore, to achieve tissue-specific interference of ephrin-As, we devised a transgenic strategy based on Cre recombination-dependent expression of a 'masking' chimera consisting of the

NIH-PA Author Manuscript

NIH-PA Author Manuscript

NIH-PA Author Manuscript

extracellular domain (ECD) of EphA4 and the GPI-anchor signal sequence of ephrin-A5. Unlike the endogenous distribution of EphA4 in microdomains lacking ephrin-A, the EphA4^{ECD}-ephrinA5^{GPI} chimera is targeted to ephrin-A-rich membrane domains, where it establishes futile cis-interactions with ephrin-A (Figure 2A, B). As shown previously, the masking of ephrin-A has a dominant negative effect on reverse signaling without affecting forward EphA-mediated signaling (Figure S2M–Q) (Marquardt et al., 2005).

Trans-binding of recombinant EphA was strongly reduced in embryos that expressed EphA4^{ECD}-ephrinA5^{GPI} in all tissues following recombination driven by *EIIa::Cre*, confirming the effectiveness of the masking (Figure S2A–F). In these embryos, the nerves that extend into the dorsal hindlimbs were stunted and defasciculated (Figure S2G, H). To determine the contribution of ephrin-A reverse signaling to motor axon guidance *in vivo*, EphA4^{ECD}-ephrinA5^{GPI} expression was selectively activated in motor neurons using *Olig2::Cre* (Dessaud et al., 2007) (Figure S2I–L). In e11.5 *EphA4^{ECD}-ephrinA5^{GPI};Olig2::Cre$^{+/-}$* embryos, less motor axons grew into the dorsal branch, whereas the ventral branch was unaffected (Figure 2C–G). In these embryos, LMC$_L$ (EphA4$^+$) axons were detected in the ventral pathway of LMC$_M$ axons, suggesting that masking of ephrin-As in motor neurons causes guidance errors rather than blocking axon growth (Figure 2H–L). In support of this finding, ~27% of the ventral shank-labeled motor neurons in *EphA4^{ECD}-ephrinA5^{GPI};Olig2::Cre$^{+/-}$* embryos were misguided LMC$_L$ neurons, compared with only ~4% in controls (Figure 2N–U). The columnar organization of motor neuron cell bodies, as well as the timing and position of LMC$_L$-LMC$_M$ axon bifurcation were unaffected in *EphA4^{ECD}-ephrinA5^{GPI};Olig2::Cre$^{+/-}$* and *Efna2$^{-/-}$;Efna5$^{-/-}$* mutants (Figure 1M–O; Figure 2Q–S, data not shown).

Motor axons expressing the masking construct were still repelled by ephrin-A in a stripe assay, suggesting that adhesive trans-interactions with ephrin-As are unlikely to account for the ventral misprojections (Figure S2M–Q). Taken together, these data indicate that ephrin-A reverse signaling in motor neurons is required *in vivo* to control the topographic projection of LMC$_L$ axons into the limb (Figure 2M).

Receptor tyrosine kinase Ret co-localizes and interacts with ephrin-As

To understand how GPI-anchored ephrin-A functions as a guidance "receptor" we sought to identify co-receptor components that transmit its signals across the membrane. The *Hb9::GFP* transgene was crossed into candidate mutant lines to directly visualize motor axon phenotypes in whole-mount preparations. The analysis focused on the peroneal nerve, the main dorsal nerve of the hindlimb, because LMC$_L$ guidance phenotypes are expected to reduce the contribution of axons to the dorsal branch, leading to thinning of the peroneal nerve, or absence in the most severe cases. The length and complexity of the nerve was evaluated and embryos were assigned to three phenotypic classes (Figure 3A–D). A quantitative estimate of the phenotype was obtained by measuring GFP fluorescence of the entire nerve (Figure 3E). As a positive control, *EphA4* mutants exhibited a ~35% reduction of the peroneal nerve, in agreement with the requirement of EphA4 for LMC$_L$ navigation (Eberhart et al., 2002; Helmbacher et al., 2000). p75 and TrkB neurotrophin receptors are required for ephrin-A reverse signaling in retinal ganglion cells (Lim et al., 2008; Marler et al., 2008) and are expressed in LMC$_L$ motor axons at the time of limb innervation (Figure S3A–C, data not shown). Surprisingly, the peroneal nerve was unaffected in both *p75* and *TrkB* mutants, indicating that they are dispensable for dorsoventral pathfinding (Figure 3D, E). We therefore considered the possibility of alternative co-receptors for ephrin-A reverse signaling in motor neurons.

To identify whether novel co-receptors associate with ephrin-A2/A5 we carried out immunoprecipitation assays in transfected cell lines to detect interacting transmembrane

NIH-PA Author Manuscript

NIH-PA Author Manuscript

NIH-PA Author Manuscript

proteins within motor axons at the stage of limb innervation (Figure 3F, data not shown). We found that Ret, the tyrosine kinase receptor for GDNF, was recovered in ephrin-A2 and ephrin-A5 immunocomplexes (Figure 3F). In addition, Ret^{+} and ephrin-$A5^{+}$ puncta partially overlapped on the growth cone plasma membrane of dissociated motor neurons (Figure 3G–I′). The heterogeneous labeling pattern suggested that the membrane-distribution of ephrin-A5 and Ret is dynamic and/or regulated at the subcellular level. To further examine the relationship between these proteins we employed a Proximity Ligation Assay (PLA) (Soderberg et al., 2006) in which oligonucleotides attached to antibodies that recognize two target proteins (i.e., Ret and ephrin-A) are ligated, amplified and detected by fluorescently labeled complementary oligonucleotide probes. This method detects proteins within close proximity to each other (< 30–40 nm). Fluorescent puncta corresponding to sites of Ret/ephrin-A interaction were present on the plasma membrane of dissociated motor neurons (Figure 3J–O). Conversely, no PLA signal was detected between ephrin-A and surface-localized DCC receptor (Figure 3P–T), which did not co-immunoprecipitate with ephrin-A2/5 (Figure 3F).

Ret mediates ephrin-A reverse signaling

GDNF binds to GPI-anchored GFRα1 receptor (*Gfrα1*), which forms a co-receptor complex with Ret (Airaksinen and Saarma, 2002). Ret and GFRα1 are expressed by limb-innervating motor neurons and GDNF is expressed at the dorsoventral choice point within the hindlimb (Kramer et al., 2006) (Figure S3D–I; see Figure 6B–D). Previous studies have noted that the peroneal nerve is perturbed in *Gdnf*, *Gfra1* and *Ret* mutant embryos (Gould et al., 2008; Kramer et al., 2006) and that gradients of GDNF attract motor axons (Dudanova et al., 2010).

The co-localization of Ret and ephrin-A proteins and guidance phenotypes of *Ret* mutants are consistent with the possibility that Ret is also a co-receptor for ephrin-A reverse signaling. We first examined whether activation of ephrin-A reverse signaling altered the phosphorylation state of Ret. We carried out biochemical assays using primary sympathetic neurons derived from the rat superior cervical ganglion (SCG), as they express functional Ret, GFRα1, and ephrin-As (Damon et al., 2010; Pierchala et al., 2006). Stimulation of ephrin-A reverse signaling with EphA7-Fc increased the levels of phosphorylated (i.e., active) Ret (Figure S3BB, CC).

In agreement with previous reports, the peroneal nerve was reduced or absent in most *Ret* mutant embryos, and the severity of the phenotype was increased in *Ret;EphA4* double mutants (Kramer et al., 2006) (Figure 3D, E). The reduction in peroneal axon projections in $Ret^{-/-}$ embryos results from the misguidance of LMC_L axons into the ventral limb (Figure S3J–O). Interestingly, the LMC_L phenotype observed in $Gfra1^{-/-}$ embryos, although highly reproducible, was less severe than the phenotype of $Ret^{-/-}$ embryos (Figure 3D, E). In contrast, GDNF-dependent innervation of the cutaneous maximus and latissimus dorsi back muscles by brachial motor neurons (Haase et al., 2002), were equally affected in *Gfra1* and *Ret* mutants (Figure S3P–R). Although GFRα1 is the preferred receptor for GDNF, GFRα2 and GFRα3 can also bind GDNF with lower affinity (Airaksinen and Saarma, 2002). Nevertheless, we found little or no expression of other GFRα isoforms in LMC motor neurons at e11.5–12.5 (data not shown). The mismatch in the incidence of peroneal phenotypes in *Gfrα1* mutants compared to *Ret* mutants suggested that Ret might have *in vivo* functions in motor axon pathfinding that extend beyond its role as a GFRα1 co-receptor for GDNF-chemoattraction.

Next, we established an *in vitro* assay to monitor the motor axon growth-promoting activity of ephrin-A reverse signaling. When cultured on a control IgG-Fc substrate, lumbar LMC explants from *Hb9::GFP* transgenic mice displayed negligible axon growth. In contrast,

NIH-PA Author Manuscript

NIH-PA Author Manuscript

NIH-PA Author Manuscript

outgrowth was robust on a substrate of clustered EphA7-Fc, which binds ephrin-A and activates reverse signaling (Figure 4A, B). Staining for the general marker of neuronal processes β3-tubulin showed that GFP^+ motor neurons had enhanced responsiveness to EphA7-Fc relative to other neuronal populations contained in the explant (Figure S4A–H). This assay was applied to explants derived from mouse mutants for candidate components of ephrin-A reverse signaling. While *p75*$^{-/-}$ and *TrkB*$^{-/-}$ motor axons had normal outgrowth on EphA7-Fc (Figure 4L, M, O, P, S), this response was significantly reduced in *Ret*$^{-/-}$ explants (Figure 4E, F, S). In contrast, EphA7-Fc-induced outgrowth was not affected by mutation of *Gfra1*, the obligatory partner of Ret for GDNF signaling (Figure 4I, J, S), or addition of a blocking antibody against GDNF, thereby excluding the possibility that defective paracrine/autocrine GDNF signaling was responsible for the impaired response of *Ret*$^{-/-}$ axons (Figure 4S). Since *Ret*$^{-/-}$ explants displayed normal outgrowth on a permissive substrate (Figure 4D, H), we conclude that Ret is required to mediate the growth-promoting effect of ephrin-A reverse signaling in motor axons, but is not necessary for axonal growth per se (Figure 4R).

Ephrin-A reverse signaling is potentiated by GDNF

Since the localized source of GDNF at the base of the limb is also necessary for LMC_L guidance (Kramer et al., 2006), we tested whether GDNF modulates ephrin-A signaling in motor neurons. Outgrowth of motor axons on EphA7-Fc was strongly enhanced by co-stimulation with low doses of GDNF that do not induce outgrowth on control IgG-Fc (Figure 4C, S). This effect was specific for GDNF since other growth factors (BDNF, HGF, CNTF), whose receptors are expressed by motor neurons (Ebens et al., 1996; Ip et al., 1993; Klein et al., 1989), did not synergize with EphA7-Fc (Figure 4S). The potentiation of ephrin-A reverse signaling by GDNF was also observed with *p75*$^{-/-}$ and *TrkB*$^{-/-}$ explants, but was absent from *Ret*$^{-/-}$ and *Gfra1*$^{-/-}$ explants (Figure 4G, K, N, Q, S). These findings suggest that the synergistic effect of GDNF on ephrin-A reverse signaling is mediated by the conventional Ret/GFRα1 receptor-complex rather than an alternative GDNF-receptor (Paratcha et al., 2003).

To explore the mechanistic basis for the enhanced ephrin-A reverse signaling caused by GDNF, we examined the localization of Ret into detergent-resistant membrane compartments (lipid rafts) enriched for GPI-anchored ephrin-A and GFRα1 proteins. We found that GDNF shifted the distribution of Ret into rafts (Figure 4T–X) (Paratcha et al., 2001; Tansey et al., 2000) resulting in co-compartmentalization of Ret and ephrin-A (Figure 4W; Figure S3T–AA′). However, activation of ephrin-A reverse signaling by EphA7-Fc failed to induce a redistribution of Ret (Figure 4T, Y, Z; Figure S3Z–AA′). Thus, GDNF might facilitate ephrin-A reverse signaling indirectly, by favoring the colocalization of Ret and ephrin-A. These findings are supported by the observation that phosphorylation of Ret and its downstream signaling components ERK1/2 and Akt is enhanced by EphA7-Fc + GDNF co-stimulation (Figure S3BB–GG).

In *Ret* mutants $EphA4^+$ LMC_L axons grow into the ventral limb where repulsive ephrin-A ligands are present (Figure S3J–O) (Kramer et al., 2006). This inconsistency suggests either ephrin-A repulsion is insufficient to prevent LMC_L axons from growing ventrally, or repulsion mediated by EphA forward signaling is diminished in *Ret* mutants. The repulsive response of motor axons to ephrin-A ligands was normal in *Ret*$^{-/-}$ explants and was not influenced by GDNF (Figure S4I–P). Thus, GDNF:Ret potentiates reverse ephrin-A signaling, but does affect EphA-mediated forward signaling. It appears that repulsion via EphA forward signaling alone is insufficient to prevent LMC_L axons from entering the ventral limb.

NIH-PA Author Manuscript

NIH-PA Author Manuscript

NIH-PA Author Manuscript

GFRα1 levels influence pathfinding

We carried out immunoprecipitation assays in cells transfected to express constant amounts of Ret and ephrin-A5 with increasing levels of GFRα1 (Figure 5A). Immunoprecipitation of Ret pulled-down both ephrin-A and GFRα1. However, the amount of ephrin-A5 associated with Ret declined when the levels of GFRα1 in Ret immunocomplexes increased. These experiments do not distinguish whether Ret/GFRα1 and Ret/ephrin-A complexes are formed separately or whether ternary complexes assemble. Nevertheless, they reveal a competitive relationship between GFRα1 and ephrin-As for Ret-binding, suggesting that the levels of these proteins influence the composition of Ret-co-receptor complexes.

Immunodetection and *in situ* analysis revealed differential levels of GFRα1 in LMC motor neurons. LMC_L neurons, which use ephrin-A reverse signaling for navigation, expressed significantly lower levels of GFRα1 compared to the LMC_M (Figure 5B–D; Figure S5A–D′). Thus, the distribution of GFRα1 and Ret are inverted: LMC_L neurons are Ret^{high}/$GFR\alpha1^{low}$, whereas LMC_M cells are Ret^{low}/$GFR\alpha1^{high}$. To determine whether differential levels of GFRα1 in motor neuron subtypes is required for proper LMC axon guidance, we generated a transgenic mouse that expresses GFRα1 under the control of the motor neuron-specific Hb9 promoter, which is highly active in $GFR\alpha1^{low}$-LMC_L neurons (Figure 5E; Figure S5E–H). In *Hb9::Gfra1* embryos the levels of GFRα1 were approximately equal on LMC_L and LMC_M axons ($GFR\alpha1^{LMC(L)}$/ $GFR\alpha1^{LMC(M)}$ ~0.9) (Figure 5F–I). Strikingly, manipulation of GFRα1 levels led to significant thinning of the peroneal nerve, indicating a reduced contribution of LMC_L axons to the dorsal branch (Figure 5J, K; Figure 3D, E). In addition, dye injection in the ventral shank revealed that LMC_L axons had misprojected into the ventral hindlimb of *Hb9::Gfra1* embryos (Figure 5L–R). Other motor neuron pathways including the ventral branch of the hindlimb and the dorsal ramus directed to axial musculature were unaffected in *Hb9::Gfra1* embryos at e10.5–e13.5 (data not shown). Importantly, innervation of the cutaneous maximus and latissimus dorsi muscles by brachial motor neurons that depend on GDNF (Haase et al., 2002) was normal in *Hb9::Gfra1* embryos (Figure S3S). These findings indicate that increased expression of GFRα1 in motor neurons did not cause a general perturbation of GDNF signaling or interfere with axonogenesis.

To further examine the state of GDNF responsiveness in *Hb9::Gfra1* motor axons, we tested the response of lumbar motor explants to a point source of GDNF (Figure S6A). Wild type explants exhibited robust directional motor axon outgrowth toward GDNF-soaked beads. As expected, $Ret^{-/-}$ explants failed to respond to GDNF, whereas *Hb9::Gfra1* motor axons behaved like wild type controls (Figure S6B–G). These findings provide additional evidence that the increased level of GFRα1 in this transgenic line does not generally impair the responsiveness and sensitivity of motor neurons to GDNF. *GFRα1* null mutants and overexpression of GFRα1 both caused qualitatively similar LMC_L guidance errors (Figure 3D, E), leading us to conclude that an optimal range of GFRα1 expression needs to be maintained on LMC_L axons to ensure accurate pathfinding.

Coincidence detection of EphA and GDNF is gated by GFRα1 levels

To determine whether the cooperative interactions between EphA and GDNF were an acute response to these factors we used a Dunn chamber growth cone turning assay (Bai et al., 2011; Yam et al., 2009). In these cultures a stable diffusion gradient of factors was established and the axonal trajectory of dissociated *Hb9::GFP*$^+$ LMC neurons was monitored for 90 minutes (Figure 6A–F). To assay the interaction between ephrin-A and GDNF signaling we created concentration gradients of EphA7-Fc-alone and GDNF-alone that were subthreshold for attracting axons, but the combination of EphA7-Fc + GDNF triggered a positive turning response (Figure 6G–K). Despite these differences, general axonal growth

NIH-PA Author Manuscript

NIH-PA Author Manuscript

NIH-PA Author Manuscript

during the culture was equivalent in all conditions tested (data not shown). Since both GFRα1 and ephrin-A use Ret for signaling and compete for interaction with Ret (see above), we asked whether GFRα1 levels influence the synergistic effect of EphA7-Fc + GDNF. We found that LMC neurons from *Hb9::Gfra1* transgenics failed to respond to the gradient of EphA7-Fc + GDNF that attracts wild type motor neurons (Figure 6G, L).

DISCUSSION

The assembly of neuronal circuits depends on the ability of growing axons to resolve and integrate information from multiple sources to navigate through complex cellular environments. We found that LMC_L motor neurons are attracted synergistically when co-stimulated by cell-surface bound EphA and secreted GDNF. The intersection of these ligands defines the axon choice point at the base of the limb where Ret functions as a coincidence detector to stimulate axon growth (Figure 7). This intersectional-detector strategy entails two levels of hierarchical receptor interactions: (1) between ligand-binding GPI-anchored ephrin-A and GFRα1 that compete for binding to co-receptor Ret, and (2) between ephrin-A co-receptors Ret, p75, and TrkB that link to different intracellular signaling pathways. We propose that these hierarchies direct the context-dependent and task-specific assembly of alternative GPI-receptor/co-receptor complexes to diversify cellular signaling. Our findings suggest that signal integration through coincidence detection may emerge as a pervasive strategy to ensure temporal correlation between interconnected pathways and as a means to build combinatorial guidance codes for expanding the range and fidelity of axonal responses that are generated with a limited stimulus set.

Ephrin-A reverse signaling instructs motor axon guidance

Ephrin-A in the ventral limb provides a repulsive signal that directs $EphA4^+$ LMC_L axons dorsally (Eberhart et al., 2002; Helmbacher et al., 2000; Kania and Jessell, 2003). Because the same axons also express ephrin-A it has been proposed that ephrin-A reverse signaling could become activated by the EphA present in the dorsal limb (Iwamasa et al., 1999; Marquardt et al., 2005). Consistent with this possibility, we show that silencing of ephrin-A receptor function in motor neurons with an $EphA4^{ECD}$-ephrin-$A5^{GPI}$ chimeric protein disturbs LMC_L axon guidance. Our *in vivo* studies support a model in which the co-expressed ephrin-A and EphA receptors trigger a 'push-and-pull' response in LMC_L axons: EphA-forward signaling mediates axon repulsion from ephrin-As in the ventral limb, and ephrin-A reverse signaling mediates axon attraction toward EphAs in the dorsal limb. The push-pull effect appears to be necessary *in vivo* because we show EphA-mediated repulsion is insufficient to divert LMC_L axons from the ventral limb when ephrin-A reverse signaling is masked. Likewise, ephrin-A-attraction is insufficient to draw LMC_L axons into the dorsal limb when EphAs are masked (Kao and Kania, 2011).

Ret mediates ephrin-A reverse signaling in motor neurons

Ephrin-A reverse signaling leads to opposite responses in different neuronal subtypes: motor and vomeronasal neurons are attracted to EphA ligands whereas retinal ganglion cells are repelled (Knoll et al., 2001; Marquardt et al., 2005; Rashid et al., 2005). It is unclear whether the diverse systems that use ephrin-A recruit different co-receptors, or whether the same co-receptor links to different signal transduction machinery. Notably, p75 and TrkB have been identified as ephrin-A co-receptors for repulsive signaling in retinal neurons (Lim et al., 2008; Marler et al., 2008), while we found they are not required for attractive ephrin-A reverse signaling in motor axons. In contrast, motor neurons use Ret to mediate attractive ephrin-A signaling. Our findings support the hypothesis that the functional diversity of ephrin-A signaling is expanded by the recruitment of alternative co-receptors (Figure 7). This raises the possibility that the composition of GPI-receptor/co-receptor complexes

NIH-PA Author Manuscript

NIH-PA Author Manuscript

NIH-PA Author Manuscript

represents a combinatorial system that might be adapted to produce distinct biological outputs.

In cells that express multiple co-receptors (e.g. Ret, p75, TrkB), such as motor neurons, there appear to be hierarchical relationships that dictate which co-receptors will be engaged. When Ret is available for binding to ephrin-As it appears to be dominant over p75 and TrkB. Although this dominance might be controlled at many levels, we propose that the competition between GFRα1 and ephrin-A for Ret binding influences the composition of receptor/co-receptor complexes. GFRα1 is required for integration and amplification of GDNF and EphA attraction, but excessive levels of GFRα1 sequester Ret and free ephrin-A to bind other co-receptors, such as p75 and TrkB. This model is consistent with the observation that retinal ganglion cells display low Ret and high GFRα1 levels, a condition that should favor the assembly of ephrin-A/p75 receptor complexes for axon repulsion (Kretz et al., 2006). Paradoxically, LMC_M motor neurons express high levels of ephrin-As, raising the question why these neurons are not attracted into the dorsal limb like LMC_L neurons (Dudanova and Klein, 2011; Kao and Kania, 2011)? However, by analogy to retinal neurons, LMC_M cells express high levels of GFRα1, which might displace ephrin-A from Ret and favor the formation of ephrin-A/p75 receptor complexes that signal axon repulsion from the $EphA^+$ dorsal limb (Figure 7).

Coincidence detection of GDNF and EphA signals in motor axons

In a variety of biological processes, integration and signal-to-noise resolution are achieved through the organization of converging signaling networks into ‘coincidence detector’ systems (Bourne and Nicoll, 1993). Coincidence detection represents a means for diversifying, sensitizing, and temporally-linking signals and transforming them into a novel output. We show that motor neurons contain a coincidence detector for GDNF and EphA ligands and that these signals are integrated by Ret to generate supralinear responses for axon growth and turning. We propose that one of the mechanisms that account for synergistic interactions between GDNF and EphA signals is via GFRα1-mediated recruitment of Ret into membrane compartments where ephrin-As are also located (Figure 7).

Our findings suggest that the coincidence detection of intersecting domains of GDNF and EphA ligands is based on receptor systems with overlapping components. These receptor complexes obey hierarchical rules to determine which transmembrane co-receptor is recruited for GPI-receptor signaling and influence how different GPI-receptors coordinate their use of shared co-receptors. The use of Ret for ephrin-A reverse signaling provides a unique advantage for tuning guidance responses to two signals because its membrane localization is controlled separately from its reverse signaling with ephrin-As. Likewise, ligand detectors without signaling activity (i.e. ephrin-As, GFRαs) in combination with co-receptors (i.e. Ret, p75, TrkB) expand the possibility of forming unique types of guidance receptor complexes to provide greater flexibility in wiring the nervous system with a limited repertoire of factors.

EXPERIMENTAL PROCEDURES

Additional details on the procedures are available in the Supplementary Information.

Mouse lines

EIIa::Cre (Lakso et al., 1996) (Jax stock #003724); *Olig2::Cre* (Dessaud et al., 2007); *Hb9::GFP* (Lee et al., 2004); *Efna2* $^{+/-}$*; Efna5* $^{+/-}$ (Feldheim et al., 2000) (Jax stock #005992); *p75* $^{-/-}$ (Lee et al., 1992); *TrkB* $^{-/-}$ (Klein et al., 1993) (Jax stock #002544);

NIH-PA Author Manuscript

NIH-PA Author Manuscript

NIH-PA Author Manuscript

EphA4 $^{-/-}$ (Dottori et al., 1998); *Gfra1*$^{-/-}$ (Cacalano et al., 1998); *Ret*$^{-/-}$ (Schuchardt et al., 1994). Microinjection of linearized plasmids into pronuclei for generating *EphA4*^{ECD}-*ephrinA5*^{GPI} and *Hb9::Gfra1* transgenic mice was performed at the Salk Transgenic Core Facility. All mouse lines were maintained by crossing to CB6F1 mice.

Neurite outgrowth assays

Explants were dissected through fluorescence-guided live microdissection from the caudal portion of the LMC of e12.5 *Hb9::eGFP* embryos and cultured in motor neuron (MN) media as previously described (Gallarda et al., 2008). For neurite outgrowth assay, explants were cultured for ~20 hrs on coverslips coated with PDL/laminin^{low} (5μg/ml) supplemented with 25–30μg/ml clustered EphA7-Fc (R&D Systems), or control IgG-Fc. Coating was performed at 37°C for 3–5 hrs. When indicated, MN media was supplemented with GDNF (0.5–1ng/ml), BDNF (5ng/ml), HGF (5ng/ml), CNFT (1.5ng/ml), or neutralizing anti-GDNF antibody (#AF-212-NA) (0.5μg/ml) (all reagents were from R&D Systems). At the concentration used, the anti-GDNF antibody was found to largely inhibit the axon growth promoting effects of GDNF on EphA7-Fc substrate (data not shown).

Stripe assays

Stripes of recombinant molecules were printed as described in Hornberger et al., 1999 and coated with laminin (5 μg/ml -Figures 1 and S1- or 10μg/ml -Figures S2 and S4). For Figures 1 and S1, EphA7-Fc (10μg/ml) and IgG-Fc (3μg/ml or 10μg/ml) were clustered with 1:3 (mass concentration ratio) Cy3-conjugated anti-human IgG-Fc antibody, while ephrin-A5-Fc (3μg/ml) was clustered with non-conjugated antibody. For Figures S2 and S4, ephrin-A5 (10μg/ml) and IgG-Fc (10μg/ml) were clustered with Cy3-conjugated and non-conjugated anti-human IgG-Fc, respectively. Lumbar motor columns dissected from e12.5 embryos were cultured on stripes for 15–20 hrs in MN media supplemented with 1ng/ml GDNF.

Supplementary Material

Refer to Web version on PubMed Central for supplementary material.

Acknowledgments

We thank Laura Franco for technical assistance; Christopher Hinckley for help with two-photon imaging; Shane Andrews for help with microscopy; Shawn Driscoll for help with data analysis; Arnon Rosenthal and Buffer Fennie for *Gfra1* mice; Bennett Novitch for *Olig2::Cre* mice; Kuo-Fen Lee for *p75* mice; Martin Goulding and Andrew Boyd for *EphA4* mice; Frank Costantini for *Ret* mice; Tsung-Chang Sung, Zhijiang Chen, Kuo-Fen Lee, Yoo-shick Lim and Dennis O'Leary for ephrin-A2/5 and p75 plasmids, and helpful discussion. DB was supported by HHMI, OC by an NINDS fellowship, GB by HHMI and a Salk pioneer fellowship and SLP is an investigator with HHMI. This research was supported by NINDS grants NS054172 and NS031249 and HHMI.

References

Airaksinen MS, Saarma M. The GDNF family: signalling, biological functions and therapeutic value. Nat Rev Neurosci. 2002; 3:383–394. [PubMed: 11988777]

Bai G, Chivatakarn O, Bonanomi D, Lettieri K, Franco L, Xia C, Stein E, Ma L, Lewcock JW, Pfaff SL. Presenilin-dependent receptor processing is required for axon guidance. Cell. 2011; 144:106–118. [PubMed: 21215373]

Bonanomi D, Pfaff SL. Motor axon pathfinding. Cold Spring Harb Perspect Biol. 2010; 2:a001735. [PubMed: 20300210]

Bourne HR, Nicoll R. Molecular machines integrate coincident synaptic signals. Cell. 1993; 72(Suppl):65–75. [PubMed: 8094038]

NIH-PA Author Manuscript

NIH-PA Author Manuscript

NIH-PA Author Manuscript

Cacalano G, Farinas I, Wang LC, Hagler K, Forgie A, Moore M, Armanini M, Phillips H, Ryan AM, Reichardt LF, et al. GFRalpha1 is an essential receptor component for GDNF in the developing nervous system and kidney. Neuron. 1998; 21:53–62. [PubMed: 9697851]

Damon DH, teRiele JA, Marko SB. Eph/ephrin interactions modulate vascular sympathetic innervation. Auton Neurosci. 2010; 158:65–70. [PubMed: 20637710]

Dessaud E, Yang LL, Hill K, Cox B, Ulloa F, Ribeiro A, Mynett A, Novitch BG, Briscoe J. Interpretation of the sonic hedgehog morphogen gradient by a temporal adaptation mechanism. Nature. 2007; 450:717–720. [PubMed: 18046410]

Dickson BJ. Molecular mechanisms of axon guidance. Science. 2002; 298:1959–1964. [PubMed: 12471249]

Dottori M, Hartley L, Galea M, Paxinos G, Polizzotto M, Kilpatrick T, Bartlett PF, Murphy M, Kontgen F, Boyd AW. EphA4 (Sek1) receptor tyrosine kinase is required for the development of the corticospinal tract. Proc Natl Acad Sci U S A. 1998; 95:13248–13253. [PubMed: 9789074]

Dudanova I, Gatto G, Klein R. GDNF acts as a chemoattractant to support ephrinA-induced repulsion of limb motor axons. Curr Biol. 2010; 20:2150–2156. [PubMed: 21109439]

Dudanova I, Klein R. The Axon's Balancing Act: cis- and trans-Interactions between Ephs and Ephrins. Neuron. 2011; 71:1–3. [PubMed: 21745632]

Ebens A, Brose K, Leonardo ED, Hanson MG Jr, Bladt F, Birchmeier C, Barres BA, Tessier-Lavigne M. Hepatocyte growth factor/scatter factor is an axonal chemoattractant and a neurotrophic factor for spinal motor neurons. Neuron. 1996; 17:1157–1172. [PubMed: 8982163]

Eberhart J, Swartz ME, Koblar SA, Pasquale EB, Krull CE. EphA4 constitutes a population-specific guidance cue for motor neurons. Dev Biol. 2002; 247:89–101. [PubMed: 12074554]

Feldheim DA, Kim YI, Bergemann AD, Frisen J, Barbacid M, Flanagan JG. Genetic analysis of ephrin-A2 and ephrin-A5 shows their requirement in multiple aspects of retinocollicular mapping. Neuron. 2000; 25:563–574. [PubMed: 10774725]

Flanagan JG, Vanderhaeghen P. The ephrins and Eph receptors in neural development. Annu Rev Neurosci. 1998; 21:309–345. [PubMed: 9530499]

Gallarda BW, Bonanomi D, Muller D, Brown A, Alaynick WA, Andrews SE, Lemke G, Pfaff SL, Marquardt T. Segregation of axial motor and sensory pathways via heterotypic trans-axonal signaling. Science. 2008; 320:233–236. [PubMed: 18403711]

Gould TW, Yonemura S, Oppenheim RW, Ohmori S, Enomoto H. The neurotrophic effects of glial cell line-derived neurotrophic factor on spinal motoneurons are restricted to fusimotor subtypes. J Neurosci. 2008; 28:2131–2146. [PubMed: 18305247]

Haase G, Dessaud E, Garces A, de Bovis B, Birling M, Filippi P, Schmalbruch H, Arber S, deLapeyriere O. GDNF acts through PEA3 to regulate cell body positioning and muscle innervation of specific motor neuron pools. Neuron. 2002; 35:893–905. [PubMed: 12372284]

Helmbacher F, Schneider-Maunoury S, Topilko P, Tiret L, Charnay P. Targeting of the EphA4 tyrosine kinase receptor affects dorsal/ventral pathfinding of limb motor axons. Development. 2000; 127:3313–3324. [PubMed: 10887087]

Hornberger MR, Dutting D, Ciossek T, Yamada T, Handwerker C, Lang S, Weth F, Huf J, Wessel R, Logan C, et al. Modulation of EphA receptor function by coexpressed ephrinA ligands on retinal ganglion cell axons. Neuron. 1999; 22:731–742. [PubMed: 10230793]

Ip NY, McClain J, Barrezueta NX, Aldrich TH, Pan L, Li Y, Wiegand SJ, Friedman B, Davis S, Yancopoulos GD. The alpha component of the CNTF receptor is required for signaling and defines potential CNTF targets in the adult and during development. Neuron. 1993; 10:89–102. [PubMed: 8381290]

Iwamasa H, Ohta K, Yamada T, Ushijima K, Terasaki H, Tanaka H. Expression of Eph receptor tyrosine kinases and their ligands in chick embryonic motor neurons and hindlimb muscles. Dev Growth Differ. 1999; 41:685–698. [PubMed: 10646798]

Kania A, Jessell TM. Topographic motor projections in the limb imposed by LIM homeodomain protein regulation of ephrin-A:EphA interactions. Neuron. 2003; 38:581–596. [PubMed: 12765610]

Kao TJ, Kania A. Ephrin-Mediated cis-Attenuation of Eph Receptor Signaling Is Essential for Spinal Motor Axon Guidance. Neuron. 2011; 71:76–91. [PubMed: 21745639]

NIH-PA Author Manuscript

NIH-PA Author Manuscript

NIH-PA Author Manuscript

Klein R, Parada LF, Coulier F, Barbacid M. trkB, a novel tyrosine protein kinase receptor expressed during mouse neural development. EMBO J. 1989; 8:3701–3709. [PubMed: 2555172]

Klein R, Smeyne RJ, Wurst W, Long LK, Auerbach BA, Joyner AL, Barbacid M. Targeted disruption of the trkB neurotrophin receptor gene results in nervous system lesions and neonatal death. Cell. 1993; 75:113–122. [PubMed: 8402890]

Knoll B, Zarbalis K, Wurst W, Drescher U. A role for the EphA family in the topographic targeting of vomeronasal axons. Development. 2001; 128:895–906. [PubMed: 11222144]

Konstantinova I, Nikolova G, Ohara-Imaizumi M, Meda P, Kucera T, Zarbalis K, Wurst W, Nagamatsu S, Lammert E. EphA-Ephrin-A-mediated beta cell communication regulates insulin secretion from pancreatic islets. Cell. 2007; 129:359–370. [PubMed: 17448994]

Kramer ER, Knott L, Su F, Dessaud E, Krull CE, Helmbacher F, Klein R. Cooperation between GDNF/Ret and ephrinA/EphA4 signals for motor-axon pathway selection in the limb. Neuron. 2006; 50:35–47. [PubMed: 16600854]

Kretz A, Jacob AM, Tausch S, Straten G, Isenmann S. Regulation of GDNF and its receptor components GFR-alpha1, -alpha2 and Ret during development and in the mature retino-collicular pathway. Brain Res. 2006; 1090:1–14. [PubMed: 16650834]

Lakso M, Pichel JG, Gorman JR, Sauer B, Okamoto Y, Lee E, Alt FW, Westphal H. Efficient in vivo manipulation of mouse genomic sequences at the zygote stage. Proc Natl Acad Sci U S A. 1996; 93:5860–5865. [PubMed: 8650183]

Landmesser LT. The acquisition of motoneuron subtype identity and motor circuit formation. Int J Dev Neurosci. 2001; 19:175–182. [PubMed: 11255031]

Lee KF, Li E, Huber LJ, Landis SC, Sharpe AH, Chao MV, Jaenisch R. Targeted mutation of the gene encoding the low affinity NGF receptor p75 leads to deficits in the peripheral sensory nervous system. Cell. 1992; 69:737–749. [PubMed: 1317267]

Lee SK, Jurata LW, Funahashi J, Ruiz EC, Pfaff SL. Analysis of embryonic motoneuron gene regulation: derepression of general activators function in concert with enhancer factors. Development. 2004; 131:3295–3306. [PubMed: 15201216]

Lim YS, McLaughlin T, Sung TC, Santiago A, Lee KF, O'Leary DD. p75(NTR) mediates ephrin-A reverse signaling required for axon repulsion and mapping. Neuron. 2008; 59:746–758. [PubMed: 18786358]

Luria V, Krawchuk D, Jessell TM, Laufer E, Kania A. Specification of motor axon trajectory by ephrin-B:EphB signaling: symmetrical control of axonal patterning in the developing limb. Neuron. 2008; 60:1039–1053. [PubMed: 19109910]

Marler KJ, Becker-Barroso E, Martinez A, Llovera M, Wentzel C, Poopalasundaram S, Hindges R, Soriano E, Comella J, Drescher U. A TrkB/EphrinA interaction controls retinal axon branching and synaptogenesis. J Neurosci. 2008; 28:12700–12712. [PubMed: 19036963]

Marquardt T, Shirasaki R, Ghosh S, Andrews SE, Carter N, Hunter T, Pfaff SL. Coexpressed EphA receptors and ephrin-A ligands mediate opposing actions on growth cone navigation from distinct membrane domains. Cell. 2005; 121:127–139. [PubMed: 15820684]

Paratcha G, Ledda F, Baars L, Coulpier M, Besset V, Anders J, Scott R, Ibanez CF. Released GFRalpha1 potentiates downstream signaling, neuronal survival, and differentiation via a novel mechanism of recruitment of c-Ret to lipid rafts. Neuron. 2001; 29:171–184. [PubMed: 11182089]

Paratcha G, Ledda F, Ibanez CF. The neural cell adhesion molecule NCAM is an alternative signaling receptor for GDNF family ligands. Cell. 2003; 113:867–879. [PubMed: 12837245]

Pasquale EB. Eph-ephrin bidirectional signaling in physiology and disease. Cell. 2008; 133:38–52. [PubMed: 18394988]

Pierchala BA, Milbrandt J, Johnson EM Jr. Glial cell line-derived neurotrophic factor-dependent recruitment of Ret into lipid rafts enhances signaling by partitioning Ret from proteasome-dependent degradation. J Neurosci. 2006; 26:2777–2787. [PubMed: 16525057]

Rashid T, Upton AL, Blentic A, Ciossek T, Knoll B, Thompson ID, Drescher U. Opposing gradients of ephrin-As and EphA7 in the superior colliculus are essential for topographic mapping in the mammalian visual system. Neuron. 2005; 47:57–69. [PubMed: 15996548]

NIH-PA Author Manuscript

NIH-PA Author Manuscript

NIH-PA Author Manuscript

Schuchardt A, D'Agati V, Larsson-Blomberg L, Costantini F, Pachnis V. Defects in the kidney and enteric nervous system of mice lacking the tyrosine kinase receptor Ret. Nature. 1994; 367:380–383. [PubMed: 8114940]

Soderberg O, Gullberg M, Jarvius M, Ridderstrale K, Leuchowius KJ, Jarvius J, Wester K, Hydbring P, Bahram F, Larsson LG, et al. Direct observation of individual endogenous protein complexes in situ by proximity ligation. Nat Methods. 2006; 3:995–1000. [PubMed: 17072308]

Tansey MG, Baloh RH, Milbrandt J, Johnson EM Jr. GFRalpha-mediated localization of RET to lipid rafts is required for effective downstream signaling, differentiation, and neuronal survival. Neuron. 2000; 25:611–623. [PubMed: 10774729]

Yam PT, Langlois SD, Morin S, Charron F. Sonic hedgehog guides axons through a noncanonical, Src-family-kinase-dependent signaling pathway. Neuron. 2009; 62:349–362. [PubMed: 19447091]

NIH-PA Author Manuscript

NIH-PA Author Manuscript

NIH-PA Author Manuscript

Highlights

- Ret is a co-receptor that signals motor axon attraction via GPI-anchored ephrin-As
- Ephrin-A reverse signaling is instructive for motor axon navigation *in vivo*
- Ret integrates GDNF and EphA signaling using a coincidence detection signaling mechanism
- Co-receptor hierarchies dictate signaling outcomes for GPI-receptors in axon guidance

NIH-PA Author Manuscript
NIH-PA Author Manuscript
NIH-PA Author Manuscript

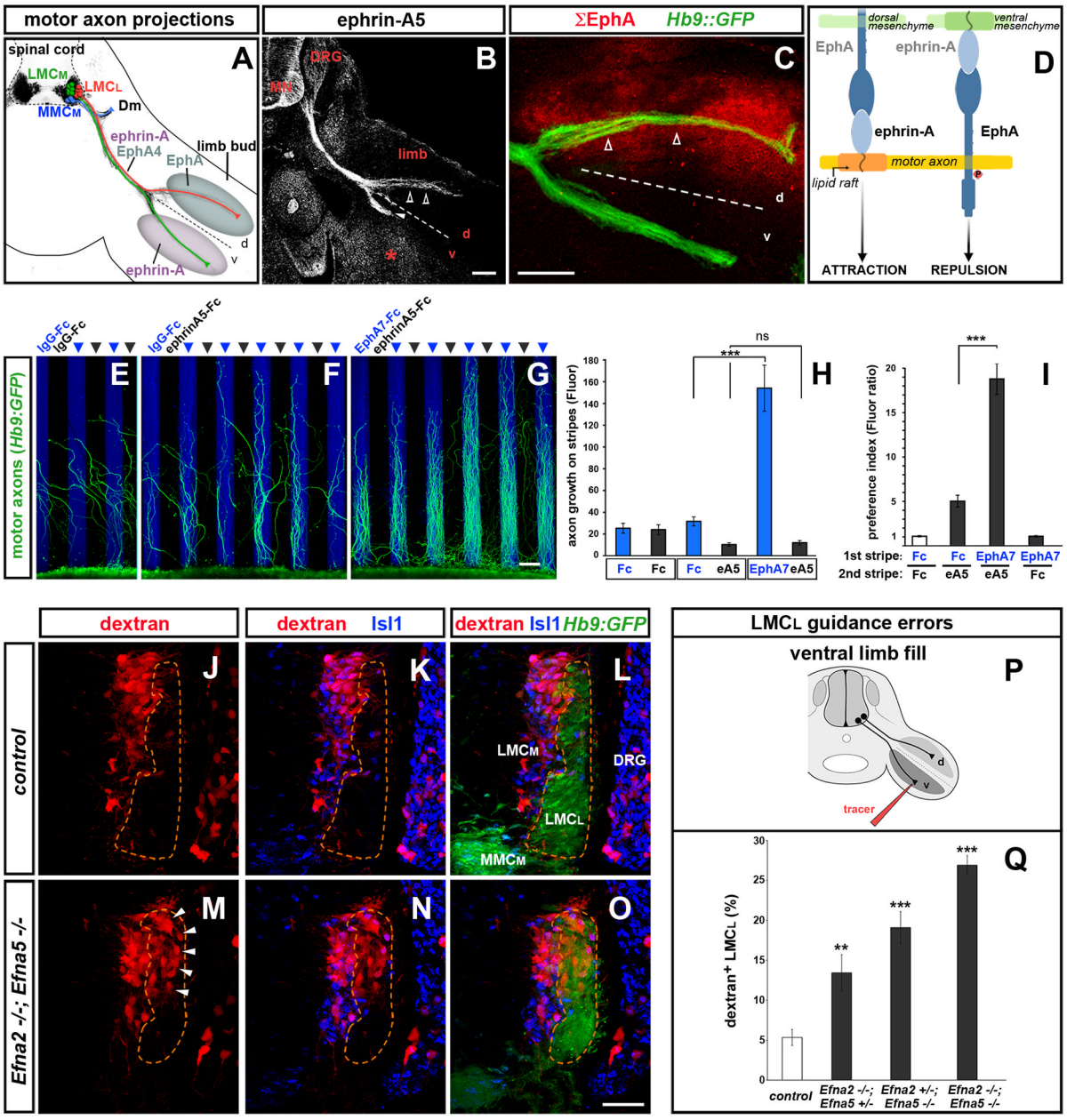

Figure 1. Coordination of forward and reverse ephrin-A signaling enhances the fidelity of axon pathway selection

(**A**) Schematic of motor neuron axon projections superimposed on transverse section of an e11.5 *Hb9::GFP*$^{+}$ (black) embryo at hindlimb level. Lateral LMC (LMC$_L$, red) and medial LMC (LMC$_M$, green) axons bifurcate at the base of the limb. Dashed line here and in following figures divides the dorsal (d) and ventral (v) halves of the limb. LMC$_L$ axons co-express EphA4 and ephrin-As, avoid ephrin-As in the ventral limb and project into the EphA-rich dorsal mesenchyme. Medial motor neurons (MMC$_M$, blue) extend to the axial musculature (demomyotome, Dm). (**B**) Ephrin-A5 staining on e11.5 LMC$_L$ axons (open arrowheads), LMC$_M$ axons (arrowhead), ventral limb mesenchyme (asterisk) and other embryonic tissues including motor neurons (MN) and dorsal root ganglia (DRG). (**C**) Cumulative distribution of EphA proteins (Σ EphA, red) in limb and motor axons detected

NIH-PA Author Manuscript

NIH-PA Author Manuscript

NIH-PA Author Manuscript

with ephrin-A5-AP on e11.5 *Hb9::GFP* embryos. LMC_L axons (open arrowheads) extend through the EphA-rich mesenchyme. (**D**) Ephrin-A reverse and forward signaling emanate from distinct membrane domains and exert opposite effects on motor axons.
(**E–I**) Stripe assay with *Hb9::GFP*$^+$ lumbar mouse motor neuron explants. (**E**) Motor axons on control IgG-Fc stripes. (**F**) Axons avoid ephrin-A5 stripes. (**G**) Axon growth is enhanced on EphA7-Fc stripes. (**H**) Quantification of GFP signal on each set of stripes. (**I**) Ratio between motor axons (GFP signal in H) on the first and second set of stripes. Mean ± SEM, N explants: IgG-Fc/IgG-Fc, 12; IgG-Fc/ephrin-A5-Fc, 11; EphA7-Fc/ephrin-A5-Fc, 12; EphA7-Fc/IgG-Fc, 10 (***) $p<0.001$; (ns) $p=0.52$ unpaired t test.
(**J–Q**) Rhodamine-dextran (red) fills of ventral-projecting motor neurons reveals LMC_L guidance errors in *Efna2/Efna5* e13.5 mutant embryos. (**J–L**) Ventral shank injection selectively labels LMC_M neurons (*Hb9::GFP*^{low}; Isl1^{high}) in WT and Hets. (**M–O**) Ventral fills in *Efna2/Efna5* mutants label LMC_M and misguided LMC_L neurons (*Hb9::GFP*^{high}; Isl1^{low}, arrowheads). (**P**) Schematic of the ventral limb fill. (**Q**) Proportion (%) of LMC_L neurons labeled by the ventral tracer. Mean ± SEM, N cells (from N embryos): *Control*, 985 (9); *Efna2*$^{-/-}$*;Efna5*$^{+/-}$, 775 (6); *Efna2*$^{+/-}$*;Efna5*$^{-/-}$, 395 (4); *Efna2*$^{-/-}$*; Efna5*$^{-/-}$, 1027 (8); (***) $p<0.001$; (**) $p<0.01$ Dunnett's test vs control.
Scale bars: A–C: 100μm; E–G: 100μm; J–O: 50μm.
See also Figure S1.

NIH-PA Author Manuscript

NIH-PA Author Manuscript

NIH-PA Author Manuscript

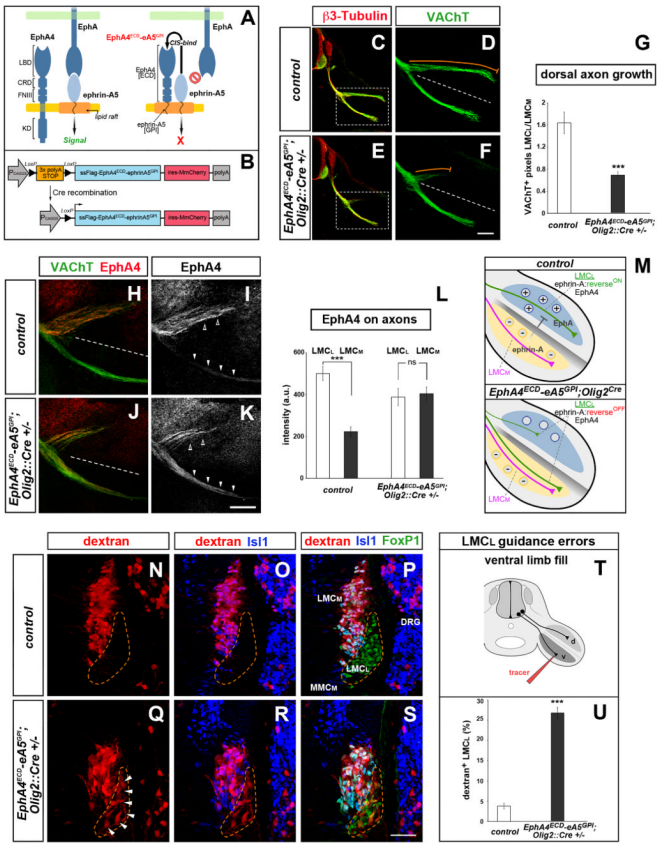

Figure 2. Ephrin-A reverse signaling is required for LMC_L dorsal limb innervation

(**A**) The $EphA4^{ECD}$-$ephrinA5^{GPI}$ chimeric masking construct is targeted to lipid rafts where it binds endogenous ephrin-As via cis-interactions. The cis-binding abolishes ephrin-Eph trans-interactions thereby blocking ephrin-A reverse signaling. (**B**) Schematic of the transgenic mouse strategy. Cre removes a 3× polyA-STOP cassette allowing expression of FLAG-tagged $EphA4^{ECD}$-$ephrinA5^{GPI}$. An internal ribosome entry site (ires) enables simultaneous translation of the monomeric, membrane-associated red fluorescent protein (RFP) MmCherry.

(**C–G**) Reduced motor axon growth into the dorsal limb at e11.5 following motor neuron-specific expression of $EphA4^{ECD}$-$ephrinA5^{GPI}$ activated by *Olig2::Cre* (orange trace adjacent to dorsal branch). The ventral motor axon appears normal. Motor neurons are marked by VAChT (green). Boxed regions in C and E are enlarged in D and F. (**G**) Ratio of $VAChT^+$ axons (LMC_L/LMC_M) in dorsal and ventral limb of transgenics and controls (WT or $Olig2::Cre^{+/-}$ littermates). Mean ± SEM, N limbs: Control, 22; Transgenic, 26; (***) $p<0.001$ unpaired t test.

(**H–M**) $EphA4^+$ LMC_L axons (open arrowheads) project exclusively to the dorsal limb in e11.5 controls, but extend in both dorsal and ventral nerve branches in $EphA4^{ECD}$-$ephrinA5^{GPI}$;$Olig2::Cre^{+/-}$ embryos (arrowheads). (**L**) Quantification of EphA4 signal in LMC_L and LMC_M axons of transgenic and control embryos. mean ± SEM, N limbs: Control, 12; Transgenic, 14 ; (***) $p<0.001$; (ns) $p=0.76$ unpaired t test. (**M**) Top, *control*: EphA in the dorsal limb mesenchyme attracts (+) while ephrin-A in the ventral limb repels (−) LMC_L axons. Bottom, $EphA4^{ECD}$-$ephrinA5^{GPI}$;$Olig2::Cre^{+/-}$: silencing of ephrin-A reverse signaling in motor neurons leads to the aberrant projection of LMC_L axons into the ventral limb.

NIH-PA Author Manuscript

NIH-PA Author Manuscript

NIH-PA Author Manuscript

(**N–P**) Rhodamine-dextran (red) injection in the ventral shank exclusively labels LMC_M neurons ($FoxP1^+$; $Isl1^+$) in control e12.5 embryos. (**Q–S**) Ventral fills in *EphA4*^{ECD}-*ephrinA5*^{GPI};*Olig2::Cre*$^{+/-}$ transgenic embryos labels LMC_M and misguided LMC_L neurons ($FoxP1^+$; $Isl1^-$, arrowheads). (**T**) Schematic of the ventral fill experiment. (**U**) Proportion (%) of LMC_L neurons labeled by the ventral tracer. Mean ± SEM, N cells (from N embryos): Control, 1179 (15); Transgenic, 1538 (11); (***) $p<0.001$ unpaired t test. Scale bars: C, E: 200μm; D, F: 100μm; H–K: 100μm; N–S: 50μm.
See also Figure S2.

NIH-PA Author Manuscript

NIH-PA Author Manuscript

NIH-PA Author Manuscript

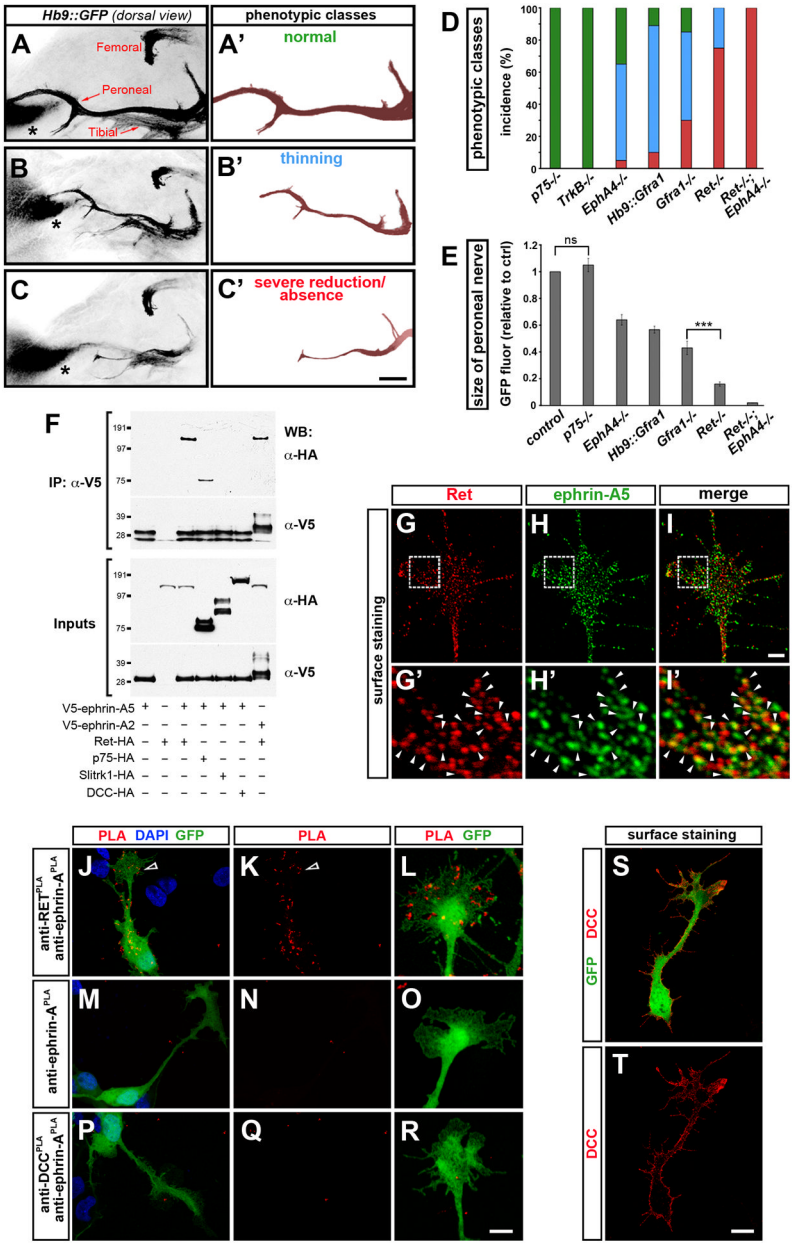

Figure 3. Genetic studies of dorsal limb innervation and Ret association with ephrin-A

(**A–C**) Dorsal view of motor axon projections into the hindlimb of whole-mount e12.5 mouse embryos (*Hb9::GFP*$^{+}$, black). The dorsal peroneal nerve and ventral tibial nerve arise from the sacral (sciatic) plexus, while the dorsal femoral nerve extends from the more rostral lumbar (femoral) plexus. The non-neuronal site of GFP expression in the dorsal limb (asterisk) serves as a reference for comparing nerve growth between embryos. (**A′–C′**) Peroneal nerve shown in isolation with examples of phenotype classes. (**D**) Incidence of the phenotypic classes in mutants (green, normal; blue, thinning; red: severe reduction/absence). (**E**) Quantification of GFP signal from the entire peroneal nerve in mutant embryos normalized to controls (mix of WT and Het littermates). Mean ± SEM, N limbs: *Control*, 110; *p75*$^{-/-}$, 20; *TrkB*$^{-/-}$, 25; *EphA4*$^{-/-}$, 50; *Hb9::Gfra1*, 70; *Gfra1*$^{-/-}$, 30; *Ret*$^{-/-}$, 60; *Ret*$^{-/-}$;*EphA4*$^{-/-}$, 10; (ns) p=0.41 *p75*$^{-/-}$ vs control; other mutants were significantly

NIH-PA Author Manuscript

NIH-PA Author Manuscript

NIH-PA Author Manuscript

different from control: p<0.001 Dunnett s test; (***) p<0.001 *Gfra1*$^{-/-}$ vs *Ret*$^{-/-}$, unpaired t test. The femoral nerve that innervates proximal dorsal muscles was unaffected in all the mutant genotypes analyzed.

(**F**) Immunoprecipitation (IP) of V5-tagged ephrin-A2 and ephrin-A5 proteins in AD293 cells followed by Western blot (WB). Ephrin-A5 and ephrin-A2 interact with Ret. Ret was recovered with higher efficiency from ephrin-A immunocomplexes than positive control p75. Ephrin-A5 does not associate with Slitrk-1 or DCC.

(**G–I′**) Colocalization of Ret and ephrin-A5 (arrowheads) on the growth cone of non-permeabilized chick motor neurons transfected with tagged proteins [Pearson's colocalization coefficient: 0.57±0.02, N=20 growth cones]. Boxed area in G–I is enlarged in G′–I′.

(**J–R**) Detection of Ret (transfected) and ephrin-A (endogenous) in close-association by PLA (red) on the surface of non-permeabilized GFP^{+} chick motor neurons (arrowheads mark growth cone). Only sporadic background signal is visible in negative controls: (**M–O**) anti-Ret antibody is omitted; (**P–R**) PLA between DCC and ephrin-A in DCC-transfected neurons.

(**S, T**) The anti-DCC antibody used in P–R detects the receptor on the surface of DCC-transfected, non-permeabilized GFP^{+} chick motor neurons.

Scale bars, A–C′: 200μm; G–I: 2μm; G′–I′: 0.44μm; J,K,M,N,P,Q,S,T: 10μm; L,O,R: 4.3μm.

See also Figure S3.

NIH-PA Author Manuscript
NIH-PA Author Manuscript
NIH-PA Author Manuscript

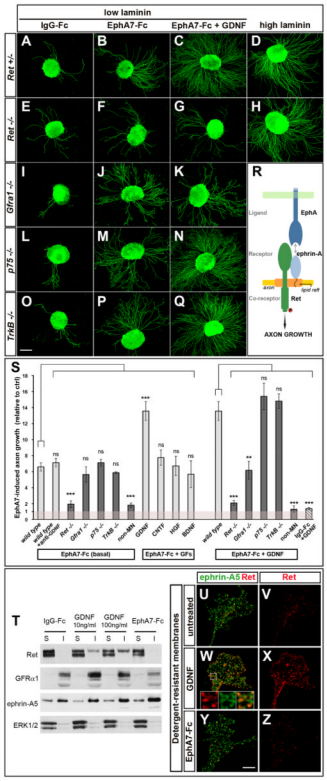

Figure 4. Ret mediates attractive ephrin-A reverse signaling

(**A–Q**) *Hb9::GFP*$^{+}$ lumbar LMC mouse motor neurons cultured on control IgG-Fc or EphA7-Fc (low laminin), in the presence or absence of GDNF. Ephrin-A reverse signaling is activated by the EphA7-Fc substrate. (**A, B, E, F**) Axonal growth stimulated by ephrin-A reverse signaling is impaired in *Ret*$^{-/-}$ explants; but is intact in (**I, J**) *Gfra1*$^{-/-}$, (**L, M**) *p75*$^{-/-}$, (**O–P**) and *TrkB*$^{-/-}$ explants. (**C, N, Q**) GDNF potentiates the growth-promoting effects of EphA-Fc in control, *p75*$^{-/-}$ and *TrkB*$^{-/-}$ explants. (**G, K**) GDNF fails to enhance axonal growth on EphA-Fc with *Ret*$^{-/-}$ and *Gfra1*$^{-/-}$ explants. (**D, H**) *Ret*$^{-/-}$ neurite outgrowth on a permissive substrate (high laminin) is unaffected.

(**R**) Schematic: Ret mediates ephrin-A reverse signaling that promotes motor axon growth.

(**S**) Quantification of the outgrowth of GFP^{+} motor axons on EphA7-Fc relative to control IgG-Fc in basal media or with growth factors (GFs) [GDNF, CNTF, HGF, BDNF] or anti-GDNF antibody. Light bars are control explants (WT and Het mutants), and dark bars mutants. ‘non-MN’ corresponds to GFP^{-} axons (see Figure S4D, H). The wild type/EphA7+GDNF bar is duplicated from the EphA7-Fc+GFs condition to facilitate comparison. The striped bar shows motor axon growth on IgG-Fc in the presence of GDNF. Number of explants on (IgG-Fc) and [EphA7-Fc] substrates. Basal MN media: Control genotypes, (63)/[69]; *Ret*$^{-/-}$ (58)/[59]; *Gfra1*$^{-/-}$ (16)/[17]; *p75*$^{-/-}$ (18)/[35]; *TrkB*$^{-/-}$ (9)/[14]; ‘non-MN’ (15)/[15]. GDNF media: Control, (51)/[82]; *Ret*$^{-/-}$ (33)/[34]; *Gfra1*$^{-/-}$ (13)/[12]; *p75*$^{-/-}$ (61)/[74]; *TrkB*$^{-/-}$ (10)/[12]; ‘non-MN’ (32)/[33]. Other treatments: anti-GDNF (10)/[12]; CNTF (6)/[10]; HGF (12)/[13]; BDNF (7)/[8]. (ns) $p>0.05$; (**) $p<0.01$; (***) $p<0.001$ Dunnett’s test vs WT in either EphA7-Fc (basal) or EphA7-Fc+GDNF conditions.

(**T**) Triton X-100 soluble (S) and insoluble (I) fractions prepared from MCF-7 cells expressing endogenous Ret and GFRα1 and transfected V5-ephrin-A5. Ephrin-A5 and GFRα1 are enriched in the detergent-resistant I fraction. Ret is recruited to the I fraction after GDNF stimulation (10ng/ml or 100ng/ml for 20min) but not after EphA7-Fc

NIH-PA Author Manuscript

NIH-PA Author Manuscript

NIH-PA Author Manuscript

stimulation (5μg/ml for 20min). Enrichment of the cytoplasmic protein ERK1/2 in the S fraction serves as a control.
(**U–V**) In resting conditions, Ret is associated with detergent-soluble membranes. (**W–X**) GDNF stimulation (50ng/ml for 15min) induces the translocation of Ret into detergent-resistant rafts where it colocalizes with ephrin-A5 (insets in **W**). (**Y–Z**) Ret translocation is not observed upon EphA7-Fc stimulation (5μg/ml for 15min).
Scale bars, A–Q: 200μm; U–Z: 5μm; 1.6 μm for insets in W.
See also Figure S4.

NIH-PA Author Manuscript

NIH-PA Author Manuscript

NIH-PA Author Manuscript

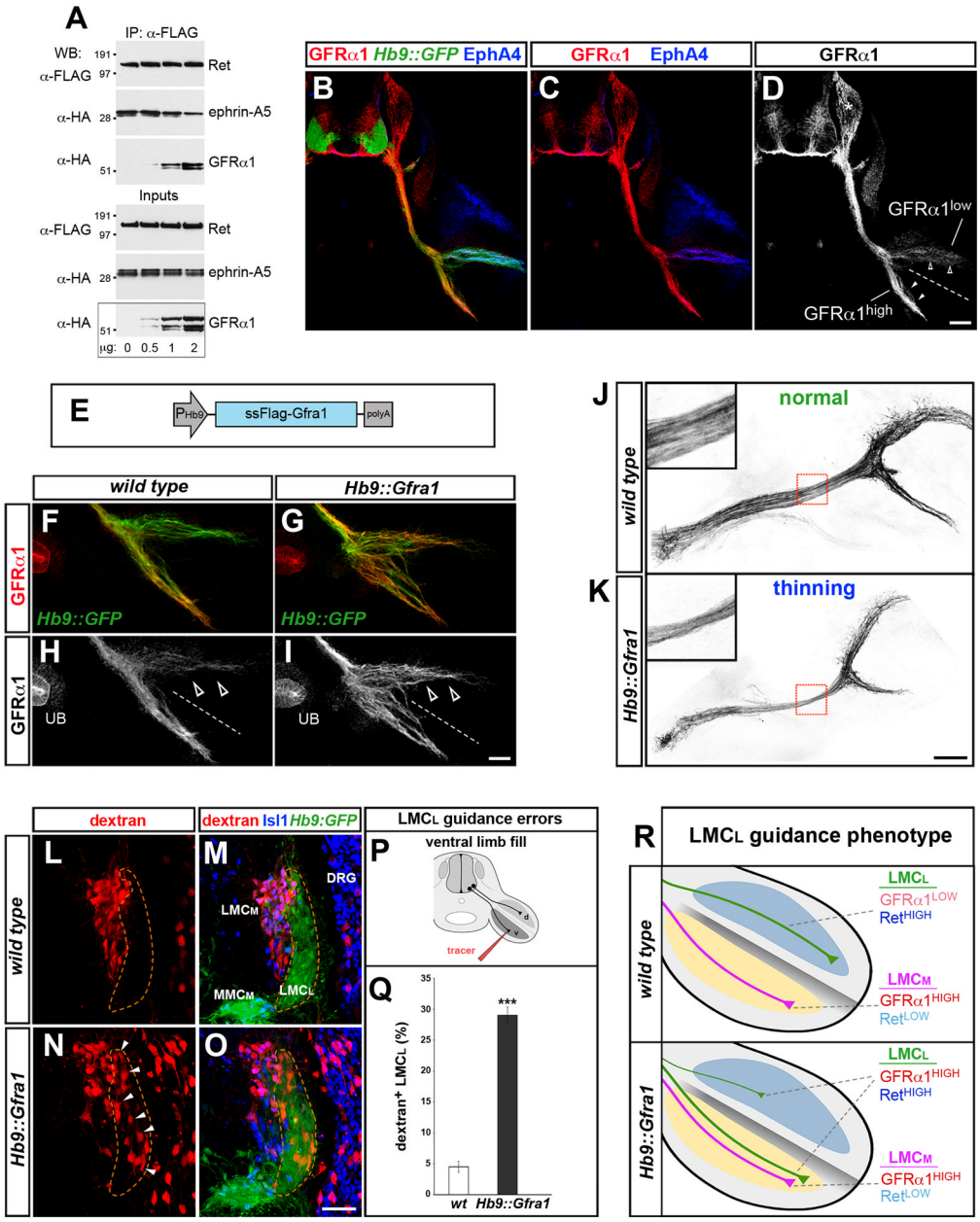

Figure 5. LMC_L axon guidance is influenced by GFRα1 levels

(**A**) AD293 cells transfected with increasing GFRα1 plasmid and constant amounts of Ret and ephrin-A5 were subjected to Ret immunoprecipitation (IP) followed by Western blot (WB) to detect Ret/ephrin-A5 and Ret/GFRα1 complexes. The relative amount of ephrin-A5 associated with Ret declines when GFRα1 is elevated. Increasing GFRα1 levels favors Ret/GFRα1 complex formation.

(**B–D**) Immunostaining of transverse sections of e11.5 *Hb9::GFP*$^+$ embryos at hindlmb level. GFRα1 is high on LMC_M axons (arrowheads) and low on EphA4$^+$ LMC_L axons (open arrowheads). GFRα1 is also expressed by sensory neurons (asterisk). The specificity of the anti-GFRα1 antibody was confirmed on *Gfra1*$^{-/-}$ sections (data not shown).

(**E**) Schematic of *Hb9::Gfra1* transgenic construct.

NIH-PA Author Manuscript

NIH-PA Author Manuscript

NIH-PA Author Manuscript

(**F–I**) GFRα1 levels increase in LMC_L axons (open arrowheads) from e11.5 *Hb9::Gfra1* embryos. GFRα1 staining in the ureteric bud (UB), which is not affected by the *Hb9::Gfra1* transgene, provides an internal standard to estimate the relative level of GFRα1 overexpression in motor axons.
(**J, K**) Dorsal views of the peroneal nerve in e12.5 whole-mount preparations (*Hb9::GFP*$^{+}$, black). Increased expression of GFRα1 in *Hb9::Gfra1* transgenics leads to thinning of the peroneal nerve. The boxed regions are enlarged in the insets. The incidence and extent of the phenotype are quantified in Figure 3D, E.
(**L–R**) Projection errors of LMC_L axons in *Hb9::Gfra1* transgenics detected by injection of rhodamine-dextran tracer (red) in the ventral shank of 13.5 embryos. (**L, M**) Ventral fills selectively label LMC_M neurons (*Hb9::GFP*^{low}; Isl1^{high}) in WT embryos. (**N, O**) Ventral fills detect misprojecting LMC_L neurons (*Hb9::GFP*^{high}; Isl1^{low}, arrowheads) in *Hb9::Gfra1* embryos. (**P**) Schematic of the ventral fill experiment. (**Q**) Proportion (%) of LMC_L neurons labeled by the ventral tracer. Mean ± SEM, N cells (from N embryos): WT, 975 (9); *Hb9::Gfra1*, 1250 (13); (***) $p<0.001$ unpaired t test. (**R**) Schematic: The levels of Ret relative to GFRα1 differ in LMC_L vs. LMC_M axons. Motor neuron-specific overexpression of GFRα1 in *Hb9::Gfra1* transgenics leads to LMC_L guidance errors.
Scale bar, A–C: 100μm; F–I: 50μm; J, K: 100μm, insets: 33μm; L–O: 50μm.
See also Figure S3S, S5, S6.

NIH-PA Author Manuscript

NIH-PA Author Manuscript

NIH-PA Author Manuscript

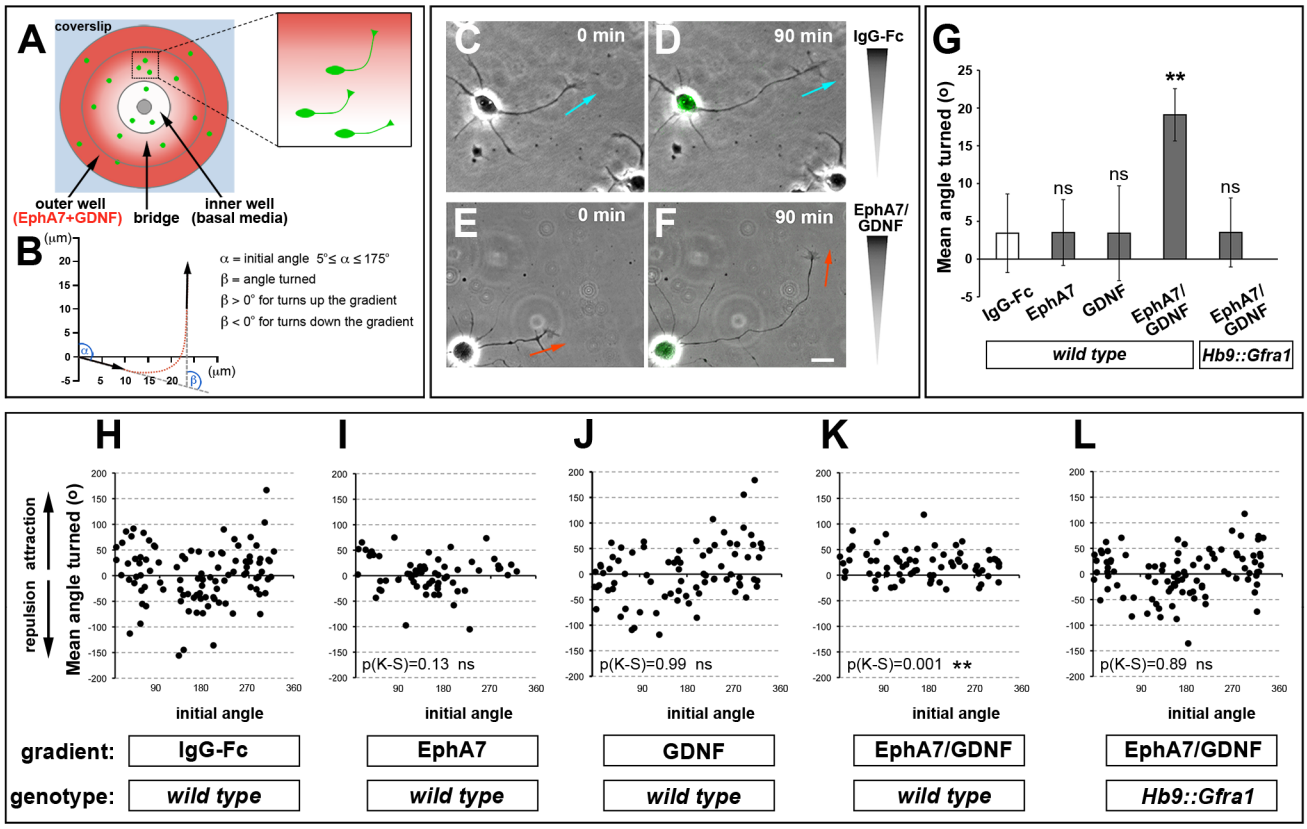

Figure 6. Coincidence detection of EphA and GDNF promotes growth cone turning and is gated by GFRα1 levels

(**A**) Top view schematic of the Dunn chamber. The inner well contains control media and the outer chamber is supplemented with guidance factors. (**B**) Method to calculate growth cone turning during 90 min. The initial angle (α) is calculated from the distal 10μm of axon relative to the gradient at t=0. The angle turned (β) is calculated from the initial and final axon trajectories. (**C–F**) Brightfield images of axons that turn toward EphA7-Fc + GDNF gradient. Axons do not turn in response to control IgG-Fc. The final images at t=90 min are superimposed on *Hb9::GFP* signal to confirm the motor neuron identity of the cells. (**G**) Mean angle turned (β ± SEM) in the presence of various factors for WT and *Hb9::Gfra1* motor axons [(ns) p>0.05; (**) p<0.01 unpaired t test vs control IgG-Fc]. (**H–L**) Scatter plots of the angle turned β versus the initial angle α for WT motor axons in the presence of IgG-Fc (N=102 axons), EphA7-Fc (N=64), GDNF (N=80), EphA7-Fc + GDNF (N=71), or *Hb9::Gfra1* motor axons in the presence of EphA7-Fc + GDNF (N=94); (KS), Kolmogorov-Smirnov test vs control IgG-Fc: (ns) p>0.05; (**) p<0.01.

Scale bar, 10μm.

See also Figure S6.

NIH-PA Author Manuscript
NIH-PA Author Manuscript
NIH-PA Author Manuscript

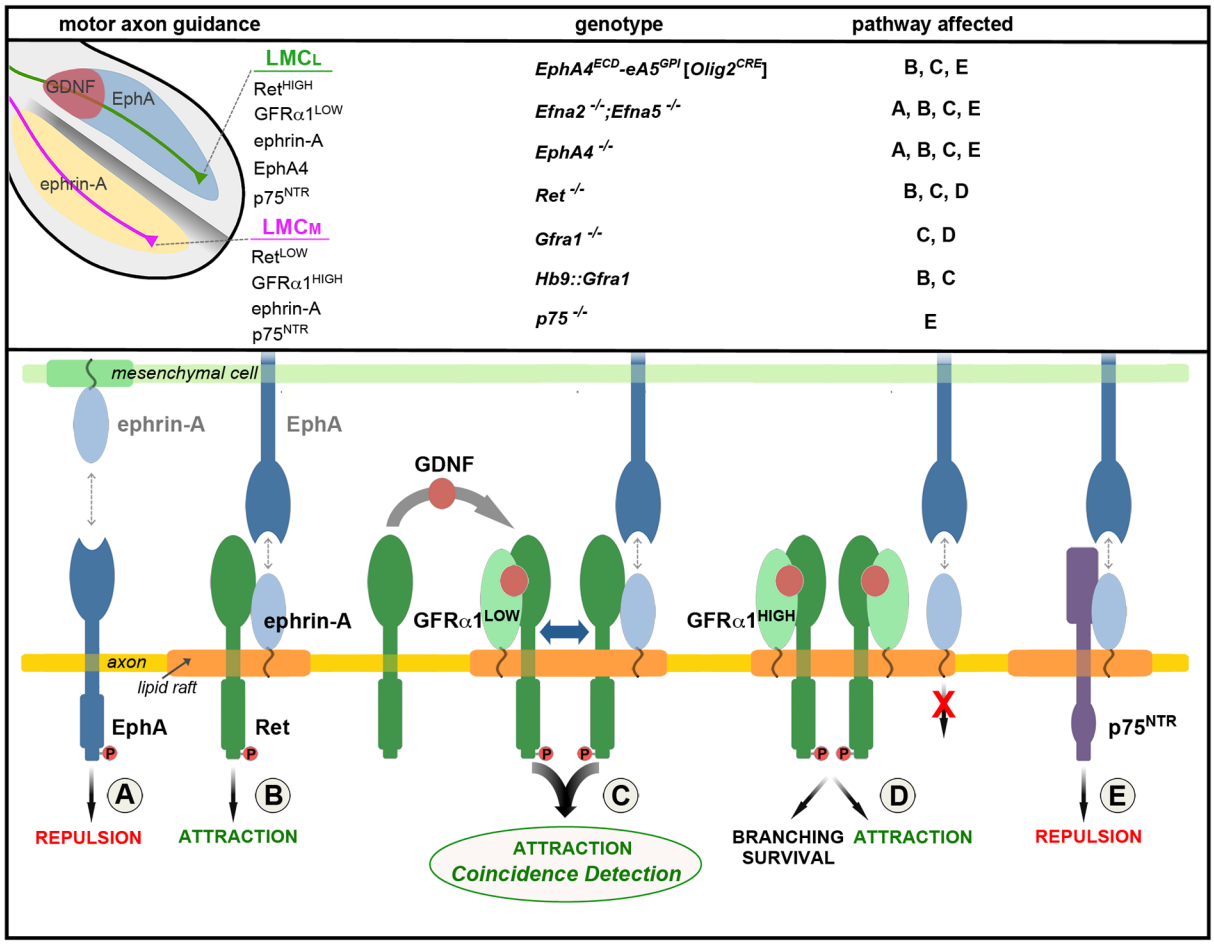

Figure 7. Model for the integration of GDNF and ephrin-A reverse signaling

(**Upper-left**) The limb is compartmentalized into a dorsal EphA$^+$ region (blue) and ventral ephrin-A$^+$ region (yellow). LMC$_L$ motor axons (green) enter the dorsal limb where the diffusible ligand GDNF (red) and transmembrane ligand EphA intersect. The expression levels of guidance receptors and co-receptors EphA4, ephrin-As, GFRα1, and Ret are different on LMC$_L$ and LMC$_M$ (purple) motor neurons. (**Upper-right**) Summary of the mouse mutants examined and the signaling pathways (A–E, lower panel) affected by each mutation. (**Lower**) The assembly of receptor/co-receptor complexes with different signaling properties depends on the relative level of the components and their distribution within the membrane. Homo-dimerization and higher-order interactions are likely, but monomers are shown for simplicity. (A) Repulsive EphA forward signaling activated by trans-binding to ephrin-As in the ventral limb. (B) Ret mediates attractive ephrin-A reverse signaling that is activated by EphAs expressed in the dorsal limb. (C) Coincidence detection and amplification of GDNF and EphA signals via GFRα1-mediated recruitment of Ret into membrane rafts where ephrin-As are also located. The co-activation of GFRα1 and ephrin-A leads to a synergistic stimulation of axon attraction that occurs when cognate ligands (GDNF, EphAs) are simultaneously encountered at the base of the dorsal limb. Together GFRα1 and ephrin-As form a coincidence detector that relies on sharing Ret for signal integration (blue double arrow). (D) High levels of GFRα1 compete with ephrin-As for binding to Ret, disrupting the co-incidence detector. GFRα1/Ret function is preserved. (E) Ephrin-A interactions with p75 produce reverse signaling for axon repulsion. This condition

exists in retinal cells (Lim et al., 2008; Marler et al., 2008) and may occur in LMC_M motor neurons where ephrin-A could be displaced from Ret by high levels of GFRα1.

NIH-PA Author Manuscript
NIH-PA Author Manuscript
NIH-PA Author Manuscript